

## ***Spitzer* Mid-IR Spectroscopy of Infrared-Luminous Galaxies at $z \sim 1 - 2$**

Lin Yan

*Spitzer Science Center, Caltech MS 220-6, Pasadena, CA 91125, USA*

**Abstract.** I discuss *Spitzer* GO programs aimed at studying the mid-IR spectral properties of IR-luminous galaxies at high  $z$ . I present the IRS low-resolution, mid-IR spectra of a sample of 52 sources from our GO1 medium size program. We found that  $\sim 75\%$  of the sample are at  $z \sim 1.5 - 2.6$ , with redshifts determined based on features including PAH emission and silicate absorption in the mid-IR spectra. This dataset revealed the first direct evidence that PAH features are already a significant component of a dusty galaxy's spectrum as early as  $z = 2$ . Among the 52 targets, one third are starbursts at  $z \sim 2$  with strong PAH emission, and two thirds are AGN-dominated systems with strong silicate absorption and weak or no PAH emission. The bulk of the sample are dusty, infrared-luminous galaxies at  $z \sim 1 - 3$  with estimated  $L_{\text{bol}} \sim 10^{13} L_{\odot}$ . At such a high luminosity, a significant fraction of our sample have dust-obscured, strong AGN components. I will discuss the implication for  $24 \mu\text{m}$ -selected, 1 mJy or brighter samples. I also present the ground-based near-IR/optical spectroscopy and 1.2 mm continuum followup observations of this sample. The Keck spectroscopic redshifts confirm the redshift measurements based on the mid-IR spectra. Since half of our sample are optically faint sources with  $R \geq 25.5 \text{ mag}$  (Vega), our results demonstrate the potential of using mid-infrared spectroscopy, especially the aromatic and silicate features produced by dust grains, to directly probe optically faint and infrared-luminous populations at high redshift.

### **1. Introduction**

Numerous studies over the past decade have found that star-forming galaxies have undergone strong evolution in their luminosity and number density since redshifts of  $1 - 2$ , and that luminous and ultraluminous infrared galaxies play a critical role in this evolution. The peak of the far-infrared background detected by *COBE* is at  $\sim 200 \mu\text{m}$ , with energy comparable to the optical/UV background (Puget et al. 1996; Fixsen et al. 1998). This implies that  $\sim 50\%$  of the integrated rest-frame optical/UV emission in the universe has to be thermally reprocessed by dust and radiated in the mid to far-infrared. Using the stacking technique, Dole et al. (2006) have recently quantified that  $24 \mu\text{m}$  sources with  $S_{24 \mu\text{m}} \sim 0.1 - 0.5 \text{ mJy}$  dominate the CIB emission at 70 and  $160 \mu\text{m}$ . Deep *ISO*  $15 \mu\text{m}$  number counts, and more recently, *Spitzer*  $24 \mu\text{m}$  number counts, suggest a large excess of mid-IR sources compared to the predictions of nonevolving models (Gruppioni et al. 2002; Marleau et al. 2004; Papovich et al. 2004). The *Spitzer*  $24 \mu\text{m}$  number counts in particular imply that a significant population of sources with flux densities of order  $100 \mu\text{Jy}$  are likely infrared-luminous galaxies at  $z \sim 1 - 3$ , previously undetected in the *ISO* data. Furthermore, the strong evolution of infrared-luminous galaxies at  $z \lesssim 1$  was directly characterized by

the infrared luminosity functions (LFs) from studies of *ISO* 15  $\mu\text{m}$  sources, and more recently *Spitzer* 24  $\mu\text{m}$  sources, with optical redshifts (Elbaz et al. 1999; Serjeant et al. 2000; Le Floc'h et al. 2005). The LF determined recently from *Spitzer* data has shown that the turn-over of the LF, which marks the dominant contributors to energy density, moves higher with redshift: the knee of the infrared LF is at  $L_{\text{IR}} \sim (3 - 5) \times 10^{11} L_{\odot}$  at  $z \sim 1$  and  $(3 - 5) \times 10^{12} L_{\odot}$  at  $z \sim 2$ . The integrated luminosity density (thus SFR) is also a function of redshift and infrared luminosity. At  $z \sim 1$ , galaxies with  $L_{\text{IR}} \geq 10^{11} L_{\odot}$  are responsible for  $70 \pm 15\%$  of the total (UV+IR) luminosity density (Le Floc'h et al. 2005). In addition, optical spectroscopy of optically faint, radio-selected,  $S_{850} > 6$  mJy submillimeter galaxies has found that these sources are at a median redshift of 2.3 (Chapman et al. 2003, 2005). Their inferred volume density,  $\sim 1.3 \times 10^{-5} \text{ Mpc}^{-3}$  at  $L_{\text{IR}} \geq 4 \times 10^{12} L_{\odot}$ , is roughly two to three orders of magnitude higher than the local density of *IRAS* ultraluminous galaxies at a similar luminosity limit (Soifer et al. 1987).

Although *ISO* and sub-mm observations have revealed many tantalizing facets of the dusty universe at  $z \sim 1 - 3$ , the successful launch of *Spitzer*, with its combined fast photometric mapping and spectroscopic capabilities, has made it possible to discover and characterize large numbers of dusty, infrared-luminous galaxies at cosmologically interesting redshifts. Of critical significance is that the mid-IR spectroscopic properties of infrared-luminous galaxies at  $z > 0.5$  are virtually unknown. The mid-IR spectra of starburst galaxies and most ULIRGs are dominated by the emission and absorption features of dust grains. While the shape of the mid-IR continuum and its brightness relative to the far-infrared constrain the amounts of hot and cold dust, the strong PAH emission features at 6.2, 7.7, 8.6, 11.3, and 12.7  $\mu\text{m}$  and silicate absorption features (centered at 9.7 and 18  $\mu\text{m}$ ) provide both an indication of the type of source heating the dust (since PAHs are easily destroyed by UV photons and X-rays from an AGN) and redshift estimates for sources that are completely obscured at shorter wavelengths (Rigopoulou et al. 1999; Genzel & Cesarsky 2000; Laurent et al. 2000; Tran et al. 2001; Draine 2003).

The local infrared-luminous galaxies show a large diversity in their mid-IR spectra; see Figure 1 in Spoon et al. (2005). With the sensitivity and wavelength coverage of the InfraRed Spectrograph (IRS; Houck et al. 2004) on *Spitzer*, it is now possible to obtain the mid-IR spectral diagnostics of dusty galaxies out to  $z \sim 3$ . The existing *Spitzer* programs studying mid-IR spectra of high-*z* IR galaxies primarily target sources with relatively bright 24  $\mu\text{m}$  fluxes, on the order of 1 mJy. Samples are either based on 24  $\mu\text{m}$ -selected targets or selected based on different wavelengths, such as sub-mm/mm or *ISO*. The 24  $\mu\text{m}$ -selected surveys include GTO programs Houck et al. (2005; 30 spectra,  $S_{24} > 0.75$  mJy,  $z \sim 2$ ) and Weedman et al. (2006, 18 spectra,  $S_{24} > 1$  mJy,  $z \sim 2$ ), and the GO programs of Le Floc'h (12 spectra,  $S_{24} > 1$  mJy,  $z \sim 0.5 - 1.5$ ), Dole et al. (16 spectra,  $z < 0.5$ ), Lagache et al. (40 spectra,  $S_{24} > 1$  mJy,  $z \sim 0.1 - 0.5$ ), Yan et al. (2005, 2007; 52 spectra,  $S_{24} > 1$  mJy,  $z \sim 1.5 - 2.6$ , GO1), and Yan et al. (152 spectra,  $S_{24} > 1$  mJy,  $z \sim 1$ , GO2). The IRS studies of high-*z* sources also include SCUBA-selected samples, such as Lutz et al. (2005a; GO1), Blain et al. (in progress, GO2), Chary et al. (in progress, GO2), and the Pérez-Fournon et al. sample of 53 bright *ISO* 15  $\mu\text{m}$  sources ( $S_{15 \mu\text{m}} > 1$  mJy). In this talk, I

will review the results from the GO1 Yan et al. program, which focuses on the mid-IR spectroscopy of IR-luminous galaxies at  $z \gtrsim 1$ .

## 2. IRS Observations of High- $z$ , Infrared-Luminous Galaxies in the FLS

### 2.1. Sample Selection

We discuss the initial results from our GO1 program, which has obtained low-resolution, mid-infrared spectra of a sample of 52 galaxies in the *Spitzer* First Look Survey (FLS)<sup>1</sup> over an area of  $3.7 \text{ deg}^2$ . The targets are potential starburst candidates at  $z \gtrsim 1 - 2$  based on their mid-IR colors. The *Spitzer* data used for our target selection are the  $24 \text{ } \mu\text{m}$  and  $8 \text{ } \mu\text{m}$  catalogs from the FLS main survey region (Fadda et al. 2006; Marleau et al. 2004; Lacy et al. 2005). In order to obtain good quality IRS spectra in reasonably short integration times, we required that all spectroscopic targets be brighter than  $0.9 \text{ mJy}$  at  $24 \text{ } \mu\text{m}$ . We applied additional color constraints in order to select potential starburst galaxies at  $z > 1$ . This is based on  $24/8$  and  $24/0.7 \text{ } \mu\text{m}$  colors. Here we define  $R(24, 8) \equiv \log_{10}(\nu f_{\nu}(24 \text{ } \mu\text{m})/\nu f_{\nu}(8 \text{ } \mu\text{m}))$ , and  $R(24, 0.7) \equiv \log_{10}(\nu f_{\nu}(24 \text{ } \mu\text{m})/\nu f_{\nu}(0.7 \text{ } \mu\text{m}))$ . The criteria used to select the IRS targets are  $R(24, 8) \geq 0.5$  and  $R(24, 0.7) \geq 1.0$ . These color cuts are determined by comparing the observed  $24/8$  and  $24/0.7 \text{ } \mu\text{m}$  color distributions of *all*  $24 \text{ } \mu\text{m}$  sources over the FLS region with the computed color tracks as a function of redshift using a set of known mid-IR spectral templates. A detailed discussion of the mid-IR color distributions in the FLS has been published in Yan et al. (2004). The  $R(24, 0.7) \geq 1.0$  condition is a crude redshift selection, and the  $R(24, 8) \geq 0.5$  cutoff selects sources with very steep, red continua. Due to the limited number of hours available to our program, we chose 52 targets at random from the total of 59 sources. The observations are taken in low resolution with the IRS.

### 2.2. Results

Of the total of 52 sources, we were able to derive redshifts for 41 based on PAH emission and/or silicate absorption features. The 52 spectra are classified into four groups, with group 1 (strong PAH) containing 16 sources, group 2 (strong silicate absorption and weak PAH) 17, group 3 (weak emission and absorption) 7, and group 4 (power-law) 12. Figure 1 shows 4–5 examples of the IRS spectra for each of these 4 groups. We mark the PAH emission at  $6.2$ ,  $7.7$ ,  $8.6$ ,  $11.2$ , and  $12.7 \text{ } \mu\text{m}$ , and the broad absorption trough roughly centered at a rest-frame wavelength of  $9.7 \text{ } \mu\text{m}$ . The redshift distribution for the full sample is shown in the left panel of Figure 2. The IRS spectra show that a large fraction of our sample (75%) are HyLIRGs with  $L_{\text{IR}} \sim 10^{13} L_{\odot}$  at  $z \sim 1.5 - 2.6$ . They reveal the first direct evidence that PAH features are already a significant component of a dusty galaxy spectrum as early as  $z = 2$ . We also found some indication that the properties of IR galaxies at high  $z$  are different from those of their  $z \sim 0$  counterparts. Specifically, among the 52 targets, one

---

<sup>1</sup>See <http://ssc.spitzer.caltech.edu/fls/> for details of the FLS observation plan and the data release.

third are starbursts at  $z \sim 2$  with strong PAH emission, and two thirds are AGN-dominated systems with strong silicate absorption and weak or no PAH emission. Because the GO1 sources are color-selected, our GO2 program was designed to obtain low-resolution IRS spectra for 152 sources, a flux-limited sample with  $S_{24\mu\text{m}} \gtrsim 1 \text{ mJy}$ . The first set of observations (69 spectra) has been reduced. The redshift distribution shows that a large fraction of these sources are  $z \sim 1$  ULIRGs. Initial analysis shows that many of these  $z \sim 1$  spectra have strong PAH emission, and some have only deep silicate absorption. The GO1 and GO2 spectra provide a large dataset characterizing the mid-IR spectral properties for galaxies at  $L_{\text{IR}} \sim 10^{12}$  and  $10^{13} L_{\odot}$  at  $z \sim 1$  and 2, respectively.

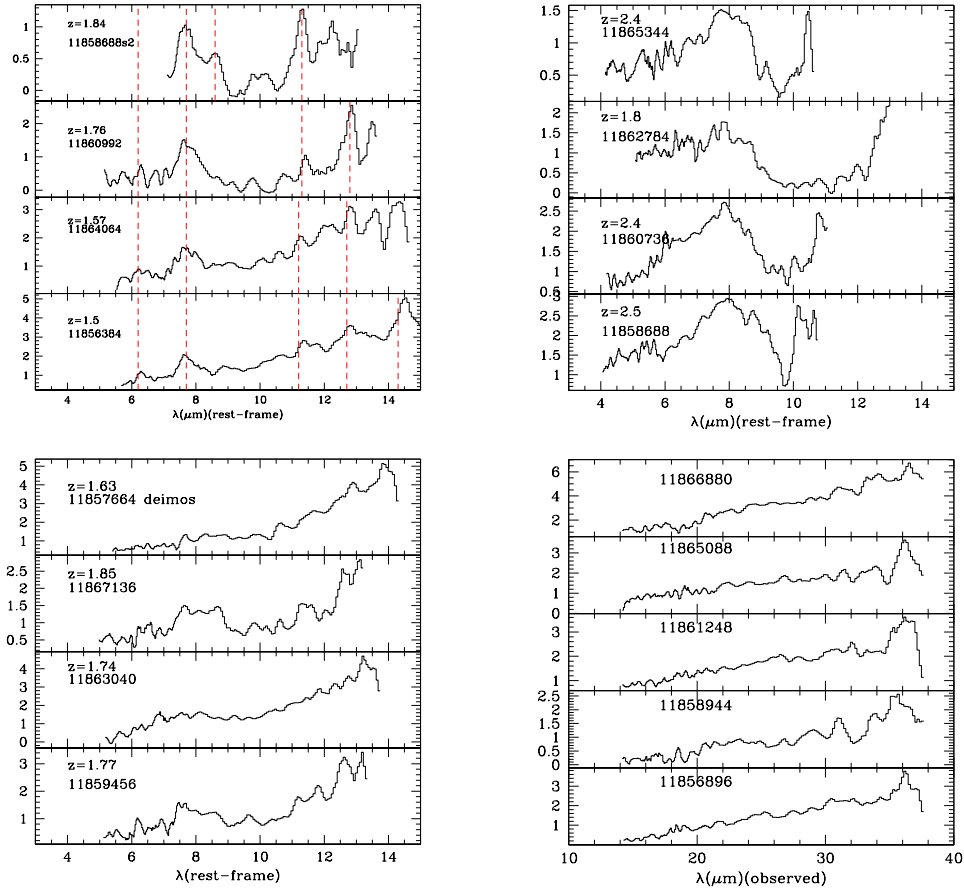


Figure 1. Upper left (a): four examples of IRS spectra with strong PAH emission (group 1). The redshift is marked at the corner of each spectrum. PAH features are marked with dashed vertical lines. Upper right (b): similar to panel (a), showing four examples of group 2 spectra with strong silicate absorption but weak or absent PAH emission. Lower left (c): similar to panel (a), showing four examples of IRS spectra with weak features, either PAH emission or silicate absorption (group 3). Lower right (d): similar to panel (a), this shows five examples of group 4 spectra, mostly power-law continua with no obvious identifiable features. No redshifts are determined for this group.

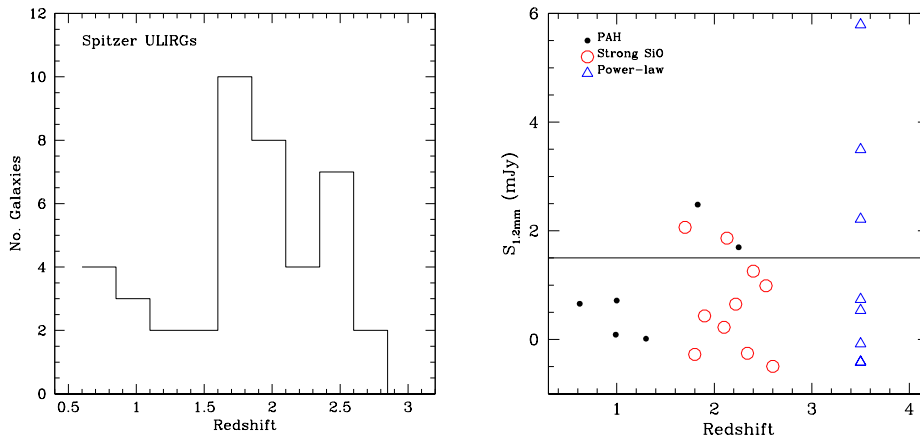


Figure 2. Left: redshift distribution of 41 of the 52-object GO1 sample. These redshifts are based purely on mid-IR spectral signatures. Right: 1.2 mm flux densities measured with MAMBO versus redshifts determined from the IRS spectra. As shown, a small fraction of our sample are detected in 1.2 mm continuum. This implies that at  $L_{\text{IR}} \sim 10^{13} L_{\odot}$ , a large fraction of  $24 \mu\text{m}$ -selected populations have dust-obscured, strong AGN components.

### 3. Millimeter Followup Observations of the GO1 Sample

We have started to obtain 1.2 mm continuum observations of the GO1 IRS sample. Half of this sample has been observed with MAMBO on the IRAM 30 m telescope. Detailed descriptions of the observations and analysis are given in Lutz et al. (2005b). The 1.2 mm sample is selected to target a subset of 40 bright ( $S_{24 \mu\text{m}} > 1 \text{ mJy}$ ) sources that are optically faint, as evidenced by a  $24 \mu\text{m}$  to optical “color”  $R(24, 0.7) \equiv \log_{10}(\nu F_{\nu}(24 \mu\text{m})/\nu F_{\nu}(0.7 \mu\text{m}))$  of at least 1.0 ( $R > 22.5$  for  $S_{24 \mu\text{m}} = 1 \text{ mJy}$ ). Each target has roughly 1.5 hours of on-source integration, with rms noise of 0.66 mJy. The sample as a whole is well-detected at mean  $S_{1.2 \text{ mm}} = 0.74 \pm 0.09 \text{ mJy}$  and  $S_{1.2 \text{ mm}}/S_{24 \mu\text{m}} = 0.15 \pm 0.03$ . Seven (three) of the sources are individually detected at  $> 3\sigma$  ( $> 5\sigma$ ) levels. Mean millimeter fluxes are higher for the sources with the reddest mid-infrared/optical colors. The right panel of Figure 2 shows the 1.2 mm fluxes versus the redshifts determined for some of the GO1 sample for which we have 1.2 mm measurements. We use different symbols for different classifications in the figure. It is clear that at the  $3\sigma$  limit of 1.98 mJy, a majority of our GO1 sources are not bright at 1.2 mm, thus do not contain tremendous amount of cold gas. This probably implies that 1 mJy or brighter  $24 \mu\text{m}$ -selected samples could include substantial AGN populations. Complete observations of the GO1 sample will be done in 2006, and we should then have better statistics on the fraction of sources with mm emission.

#### 4. Keck Optical and Near-IR Spectroscopic Followup Observations

We obtained optical and near-IR spectra for 28 sources from our IRS sample using the instruments (LRIS, DEIMOS, and NIRSPEC) on the Keck telescopes. From these data, we were able to determine redshifts for 18 of these sources. All of the Keck redshifts confirm the estimates based only on the mid-IR features, even in a few ambiguous cases where the IRS redshifts are based on weak features and slope changes in the mid-IR continua. The rest-frame UV/optical emission lines detected in the Keck spectra are mostly also consistent with the source classifications suggested by the mid-IR spectra. The detailed analyses of the optical and near-IR spectra, including line widths, nebular metallicities, optical energetic diagnostics, and star formation rate estimates, will be presented in a separate paper (Yan et al., in preparation). Here the main point is to demonstrate that our IRS redshift measurements are fairly reliable. Figure 3 shows three examples of Keck spectra, one per instrument (NIRSPEC, LRIS, and DEIMOS). For each object, we plot its IRS mid-IR data together with the Keck spectrum. Notable spectral features are marked in each panel. Of the eight sources observed by NIRSPEC, we were able to detect  $H\alpha$  emission line for six of them. The redshift range for this group of sources is  $1.8 < z < 2.6$ . The rest-frame FWHMs of the  $H\alpha$  line in all six sources are fairly narrow, less than  $1000 \text{ km s}^{-1}$ . The  $[\text{N II}]/H\alpha$  ratios are in the range 0.1–0.3, which spans the range of values for both starbursts and Seyfert 2s. Additional near-IR spectroscopy, covering both  $H\alpha$  and  $[\text{O III}] 5007$ , has been scheduled for more sources from our IRS sample. Using LRIS and DEIMOS, we were able to measure redshifts for six and five sources, respectively, mostly at  $z \sim 1$ . One source, MIPS110, has a power-law mid-IR spectrum without an IRS redshift. Its DEIMOS spectrum shows that it is an AGN at  $z = 1.0505$  (see Fig. 3). Optical and near-IR spectroscopic observations for the whole IRS sample have been planned. The complete spectral dataset, including both optical and mid-IR, will be discussed in a forthcoming paper (Yan et al., in preparation).

#### 5. Cosmological Implications

The detection of infrared-luminous galaxies at  $z \sim 2$  based on only mid-IR spectra has several significant implications for studies of galaxy evolution at high redshift. As a benchmark for comparison, the comoving number density of sub-mm detected galaxies at  $\langle z \rangle = 2.2$  and  $1 < z < 3$  is roughly  $6 \times 10^{-6} \text{ Mpc}^{-3}$  for  $L_{\text{IR}} \geq 4 \times 10^{12} L_{\odot}$  (Chapman et al. 2004), and the rest-frame UV-color selected galaxies have a comoving space density of  $2 \times 10^{-3} \text{ Mpc}^{-3}$  for both the BM ( $\langle z \rangle = 1.77$ ) and BX ( $\langle z \rangle = 2.32$ ) selections (Adelberger et al. 2004). It is worth pointing out that although optically faint, radio-selected SCUBA galaxies tend to have rest-frame UV colors satisfying the BX and BM criteria, they have much fainter  $R$ -band magnitudes (Chapman et al. 2003). Although our current sample is very small, it would be illustrative to compute the comoving number density of infrared-luminous galaxies at  $z \sim 2$ . Our crude estimate is as follows. Among all of the  $24 \mu\text{m}$  sources over the area we studied ( $3.7 \text{ deg}^2$ ), 59 sources satisfy our sample selection conditions. If we assume 75% of these 59 sources lie at  $z = 2.0 \pm 0.3$ , the comoving number density is  $n = N/V_c \sim$

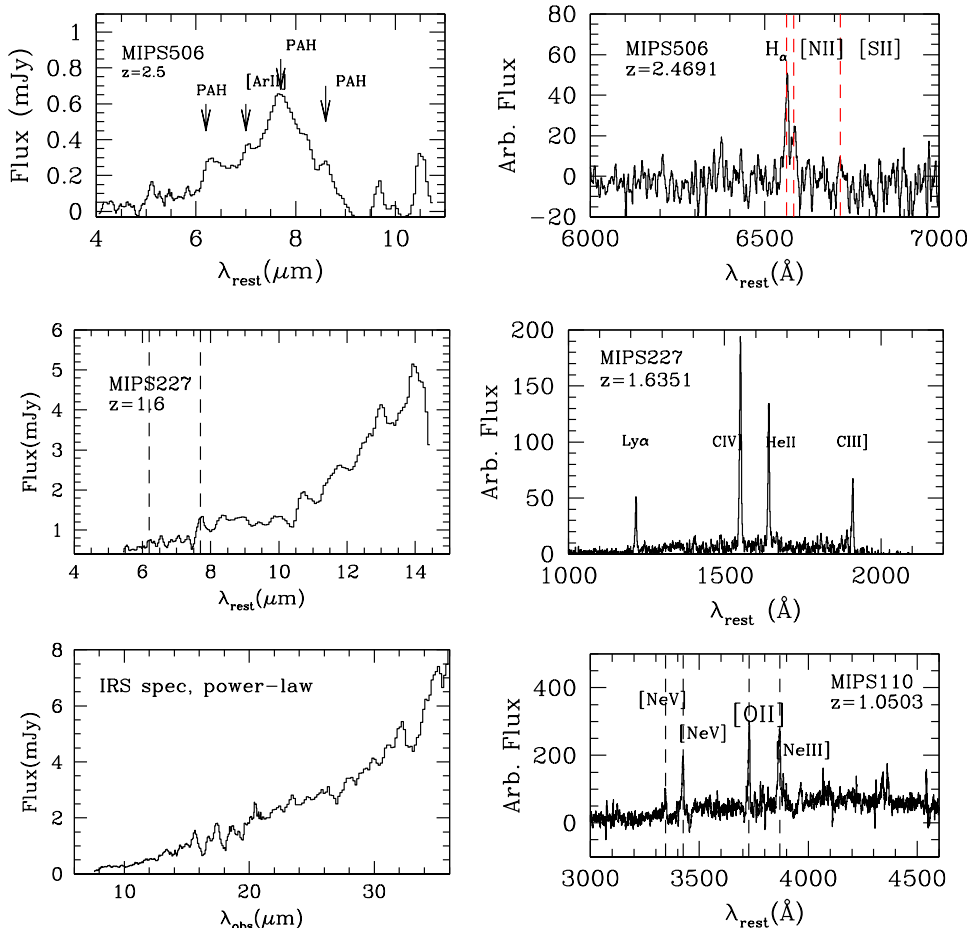


Figure 3. Three examples of Keck spectra, one for each instrument—NIR-SPEC, LRIS and DEIMOS. We plot the mid-IR data together with the Keck spectrum for each source.

$2 \times 10^{-6} \text{ Mpc}^{-3}$  for  $z = 2$  and  $L_{\text{IR}} \geq 5 \times 10^{12} L_{\odot}$ . Given the large uncertainties, our estimate is probably consistent with the density of sub-mm sources and is roughly 1% that of the UV-selected  $z \sim 2$  galaxies. The exact relation between our sample and SCUBA sources would require future work to quantify. We note that the bolometric infrared luminosity of UV selected galaxies at  $z \sim 2 - 3$  is roughly  $10^9 - 10^{10} L_{\odot}$  (Adelberger & Steidel 2000), 3–4 orders of magnitude less than those of our sources. Therefore, galaxies like those from our sample could contribute significantly to the total luminosity density at high redshift.

**Acknowledgments.** We are grateful to the IRS instrument team and the IRS instrument support team at the Spitzer Science Center for their tremendous effort to make this instrument such a great success. Support for this work was provided by NASA through award issued by JPL/Caltech. The spectroscopic data presented herein were obtained at the W. M. Keck Observatory, which is operated as a scientific partnership among the California Institute of Tech-

nology, the University of California, and the National Aeronautics and Space Administration.

## References

- Adelberger, K. L., Steidel, C. C., Shapley, A. E., Hunt, M. P., Erb, D. K., Reddy, N. A., & Pettini, M. 2004, *ApJ*, 607, 226
- Adelberger, K. L. & Steidel, C. C. 2000, *ApJ*, 544, 218
- Chapman, S., Blain, A. W., Ivison, R. J., & Smail, I. R. 2003, *Nature*, 422, 695
- Chapman, S. C., Blain, A. W., Smail, I., & Ivison, R. J. 2005, *ApJ*, 622, 772
- Chapman, S. C., Smail, I., Blain, A. W., & Ivison, R. J. 2004, *ApJ*, 614, 671
- Dole, H., et al. 2006, *A&A*, 451, 417
- Draine, B. T. 2003, *ARA&A*, 41, 241
- Elbaz, D., et al. 1999, *A&A*, 351, L37
- Fadda, D., et al. 2006, *AJ*, 131, 2859
- Fixsen, D. J., Dwek, E., Mather, J. C., Bennett, C. J., & Shafer, R. A. 1998, *ApJ*, 508, 123
- Franceschini, A., Fadda, D., Cesarsky, C. J., Elbaz, D., Flores, H., & Granato, G. L. 2002, *ApJ*, 568, 470
- Genzel, R. & Cesarsky, C. J. 2000, *ARA&A*, 38, 761
- Gruppioni, C., Lari, C., Pozzi, F., Zamorani, G., Franceschini, A., Oliver, S., Rowan-Robinson, M., & Serjeant, S. 2002, *MNRAS*, 335, 831
- Houck, J. R., et al. 2004, *ApJS*, 154, 18
- Houck, J. R., et al. 2005, *ApJ*, 622, L105
- Lacy, M., et al. 2005, *ApJS*, 161, 41
- Laurent, O., Mirabel, I. F., Charmandaris, V., Gallais, P., Madden, S. C., Sauvage, M., Vigroux, L., & Cesarsky, C. 2000, *A&A*, 359, 887
- Le Floc'h, E., et al. 2005, *ApJ*, 632, 169
- Lutz, D., Valiante, E., Sturm, E., Genzel, R., Tacconi, L. J., Lehnert, M. D., Sternberg, A., & Baker, A. J. 2005, *ApJ*, 625, 83
- Lutz, D., Yan, L., Armus, L., Helou, G., Tacconi, L. J., Genzel, R., & Baker, A. J. 2005, *ApJ*, 632, L13
- Marleau, F. R., et al. 2004, *ApJS*, 154, 66
- Papovich, C., et al. 2004, *ApJS*, 154, 70
- Puget, J.-L., Abergel, A., Bernard, J.-P., Boulanger, F., Burton, W. B., Désert, F.-X., & Hartmann, D. 1996, *A&A*, 308, L5
- Rigopoulou, D., Spoon, H. W. W., Genzel, R., Lutz, D., Moorwood, A. F. M., & Tran, Q. D. 1999, *AJ*, 118, 2625
- Serjeant et al. 2000, *MNRAS*, 317, 29
- Soifer, B. T., Sanders, D. B., Madore, B. F., Neugebauer, G., Danielson, G. E., Elias, J. H., Lonsdale, C. J., & Rice, W. L. 1987, *ApJ*, 320, 238
- Spoon, H. W. W., Keane, J. V., Cami, J., Lahuis, F., Tielens, A. G. G. M., Armus, L., & Charmandaris, V. 2005, in *Astrochemistry: Recent Successes and Current Challenges*, ed. D. C. Lis, G. A. Blake, & E. Herbst (Cambridge: Cambridge University Press), 281
- Tran, Q. D., et al. 2001, *ApJ*, 552, 527
- Weedman, D. W., Le Floc'h, E., Higdon, S. J. J., Higdon, J. L., & Houck, J. R. 2006, *ApJ*, 638, 613
- Yan, L., et al. 2005, *ApJ*, 624, 608
- Yan, L., et al. 2004, *ApJS*, 154, 60
- Yan, L., et al. 2007, *ApJ*, 658, 778



## Discussion

*Robson:* Given the problems of redshift selection based on two-waveband photometry with significant bandwidths and objects that have broad spectral features of emission and absorption, are you confident that your selection is undersampling the lowest redshift population, especially in the 1 to 1.5 redshift range?

*Yan:* The  $24\mu\text{m}/8\mu\text{m}$  color is aimed at selecting starburst galaxies at  $z > 1$ . So the bias against low- $z$  sources is expected. The bias against  $z \sim 1.5$  sources is true, and is due to silicate absorption moving into the  $24\mu\text{m}$  band at  $z \sim 1.5$ .



Daisuke Iono and Glen Petitpas